



## Original article

## A new concept of the contraction–extension property of the left ventricular myocardium



Motono Tanaka (MD, PhD, FJCC)<sup>a,\*</sup>, Tsuguya Sakamoto (MD, PhD, FJCC)<sup>b</sup>,  
Shigeo Sugawara (MD, PhD, FJCC)<sup>a</sup>, Yoshiaki Katahira (MD, PhD, FJCC)<sup>a</sup>,  
Haruna Tabuchi (MD)<sup>a</sup>, Hiroyuki Nakajima (RMS)<sup>a</sup>, Takafumi Kurokawa (RMS)<sup>a</sup>,  
Hiroshi Kanai (PhD)<sup>c</sup>, Hideyuki Hasegawa (PhD)<sup>c</sup>, Shigeo Ohtsuki (PhD)<sup>d</sup>

<sup>a</sup> Cardiovascular Center, Tohoku Pharmaceutical University Hospital, Fukumuro 1-12-1, Miyagino-ku, Sendai 983-0005, Japan

<sup>b</sup> Hanzomon Hospital, Kojimachi 1-14, Chiyoda-ku, Tokyo 102-0083, Japan

<sup>c</sup> Department of Electrical Engineering, Tohoku University, Aramaki-Aoba 6-6-05, Aoba-ku, Sendai 980-8579, Japan

<sup>d</sup> Institute of Medical Ultrasound Technology, Yokohama 2-12-15, Sagami-hara 229-1122, Japan

## ARTICLE INFO

## Article history:

Received 12 June 2013

Received in revised form 15 August 2013

Accepted 9 September 2013

Available online 27 November 2013

## Keywords:

Myocardial contraction–Extension property

Strain rate distribution

Phase difference tracking method

Peristalsis and bellows action of the

ventricular wall

Non-uniformity of myocardial contraction

and extension

## ABSTRACT

**Objectives:** Using newly developed ultrasonic technology, we attempted to disclose the characteristics of the left ventricular (LV) contraction–extension (C–E) property, which has an important relationship to LV function.

**Methods:** Strain rate (SR) distribution within the posterior wall and interventricular septum was microscopically measured with a high accuracy of 821  $\mu\text{m}$  in spatial resolution by using the phase difference tracking method. The subjects were 10 healthy men (aged 30–50 years).

**Results:** The time course of the SR distribution disclosed the characteristic C–E property, *i.e.* the contraction started from the apex and propagated toward the base on one hand, and from the epicardial side toward the endocardial side on the other hand. Therefore, the contraction of one area and the extension of another area simultaneously appeared through nearly the whole cardiac cycle, with the contracting part positively extending the latter part and *vice versa*. The time course of these propagations gave rise to the peristalsis and the bellows action of the LV wall, and both contributed to effective LV function.

The LV contraction started coinciding in time with the P wave of the electrocardiogram, and the cardiac cycle was composed of 4 phases, including 2 types of transitional phase, as well as the ejection phase and slow filling phase. The sum of the measurement time duration of either the contraction or the extension process occupied nearly equal duration in normal conditions.

**Conclusion:** The newly developed ultrasonic technology revealed that the SR distribution was important in evaluating the C–E property of the LV myocardium. The harmonious succession of the 4 cardiac phases newly identified seemed to be helpful in understanding the mechanism to keep long-lasting pump function of the LV.

© 2013 Japanese College of Cardiology. Published by Elsevier Ltd. All rights reserved.

## Introduction

The mechanical properties of the myocardial fiber, the multi-fiber scale mechanical performance of the ventricular wall (LV), and their mutual correlations are fundamental determinants of LV function.

Although experimental studies using isolated muscle fiber or multi-cellular myocardial tissue or anesthetized animals have been published [1–8], it was difficult to obtain exact *in situ* information even from open-chest surgical operations. This is

because the hemodynamics and the flow structure will certainly be changed under the atmospheric pressure [1–8]. To date, several non-invasive trials using ultrasonic methods have been proposed [9–11], however, because of poor spatial resolution, an ideal method for clinical application has not yet been described, particularly in respect to the differential properties of the various regions of the ventricular wall.

## Objective

Our aim was to obtain information regarding the contraction extension (C–E) property of the regional myocardial tissue to investigate the mechanical performance of the LV wall. For this, we developed a new method of measurement of the myocardial strain

\* Corresponding author. Tel.: +81 022 719 5161; fax: +81 022 719 5166.  
E-mail addresses: [m.tanaka@jata-miyagi.org](mailto:m.tanaka@jata-miyagi.org), [shin@jcc.gr.jp](mailto:shin@jcc.gr.jp) (M. Tanaka).

rate (SR) with high resolution using a phase difference tracking technique [12–16]. Then, we tried to verify the precise C–E property of the myocardial tissue on the microscopic and macroscopic scales *in situ*, which had never been attempted before.

## Subjects and methods

### Subjects

Ten healthy male volunteers aged 30–50 ( $39.6 \pm 10.4$ ) years who gave informed consent were investigated.

### Methods

#### Acquisition of ventricular dynamics information

To obtain information on wall dynamics, a specially designed ultrasonic machine (Aloka 6500 model, Hitachi Aloka Medical Ltd., Tokyo, Japan) was used. In the supine or left lateral decubitus position, a transthoracic parasternal  $90^\circ$  sector scan was performed, while selecting a scanning plane passing through 3 points (centers of both the aortic and mitral orifices and the LV apex). This plane, including the center of the LV and left atrium (LA) and 2 flow (inflow and outflow) axis lines, was named “longitudinal section plane” as described in the previous paper [17]. The measurements were done on this plane to minimize the acoustical measurement error. Perpendicular to this plane is the short-axis plane.

#### Measurement of SR distribution of the myocardium

The 2D echocardiographic equipment had a pulsatile ultrasound frequency of 3.5 MHz, 4.5 kHz in repetition rate, 1.5 mm in beam width, and  $0.5 \mu\text{s}$  in pulse width. The range of the limited angle of  $30^\circ$  out of  $90^\circ$  was scanned at a high speed of 630–700 frame/s, switching 5 beam directions evenly sectioned from the base to the apex (1–5: sparse scan) (Fig. 1, top). The echo signals from the ventricular wall for about 2–6 second received in every 1–5 beam direction were recorded in the memory and processed off-line by using our own developed software [12–15].

After determining the measuring range from the endocardium to the epicardium (Fig. 1, bottom), the measuring width ( $821 \mu\text{m}$ ) was settled. Then, the velocity  $\{v(x_1), v(x_2)\}$  of the tissue at the 2 terminal moving points ( $x_1$  and  $x_2$ ) of the measuring width ( $821 \mu\text{m}$ ) was successively calculated as follows.

The phase difference between 2 successive reflection pulses at the  $x_1$  and  $x_2$  points was measured by the “quadrature demodulation”, and the velocities ( $v$ ) at these 2 points were calculated, as having a propagation velocity of 1600 m/s [18] in the myocardium.

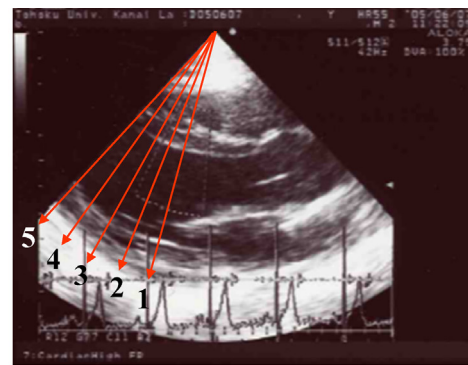
SR was calculated using the bottom equation  $\{S_i(t)\}$  [15].

The serial SR distribution in the wall was obtained by calculating the SR, while shifting the measuring width ( $821 \mu\text{m}$ ) every  $200 \mu\text{m}$  through the endocardium and the epicardium (about 10 mm). The accuracy of measurement was about  $2 \mu\text{m}$ .

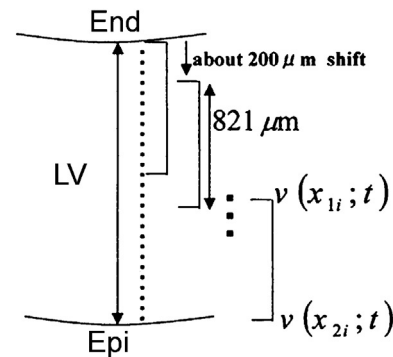
The time serial SR distribution was displayed on the M-mode image by color-coded information (Fig. 2). The serial red lines of 1–5 indicate each beam direction from the base to the apex as shown in the top of Fig. 1.

The increment of the SR (contraction) was indicated by cold color (dark to light blue tone) and the warm color indicated the decrement of the SR (extension) (red to yellow tone). In between, the black zero zone (B in Fig. 2) indicated the relaxation, where the myocardium had near zero SR.

The C–E property in the LV myocardium was evaluated by the changes in the time serial SR distribution as shown in Fig. 2.



beam number



$$\text{Strain Rate } (S_i(t)) = \frac{v(x_{2i}; t) - v(x_{1i}; t)}{|x_{2i}(t) - x_{1i}(t)|} \quad [(\text{m/s})/\text{m}]$$

**Fig. 1.** Principle of the measurement of high resolution strain rate in the myocardium using the phase difference tracking method. Top: longitudinal 2D echocardiogram to decide 5 beam directions (1 → 5; base → apex) separated by  $7.5^\circ$ . These serial numbers correspond to the numbers shown in Fig. 2. Bottom: selection of the measurement range (from epicardium = Epi to endocardium = End) and the measuring width ( $821 \mu\text{m}$ ). The velocity ( $v$ ) in the myocardial tissue at 2 terminal points ( $x_{1i}, x_{2i}$ ) are calculated, and then the strain rate is obtained by the bottom equation ( $S_i(t)$ ). LV, left ventricular wall.

## Results

The results obtained in all 10 subjects were essentially uniform. The minor difference was seen from beat to beat and among the subjects, but the general tendency was unequivocal. The heart rate gave the difference in the absolute value of the length of each phase, but there was little influence on the sequence of the SR distribution, at least among the normal subjects.

Therefore, it seemed to be enough to describe the results of one representative case in detail.

### C–E property in the LV myocardium (Fig. 2, Table 1)

The contraction and extension and also relaxation did not occur all at once, but occurred rather sporadically during one cardiac cycle. Simultaneous or synchronous contraction or extension of the whole wall muscles was never seen, and further, the C–E property of the free wall (e.g. PW) was different from that of the IVS.

### Posterior wall

The contraction of the PW started from the apical epicardial side, coinciding in time with the P wave of electrocardiogram (ECG) (indicated by the thick black arrow at bottom), and propagated toward the endocardial side during ejection phase (Ej); also

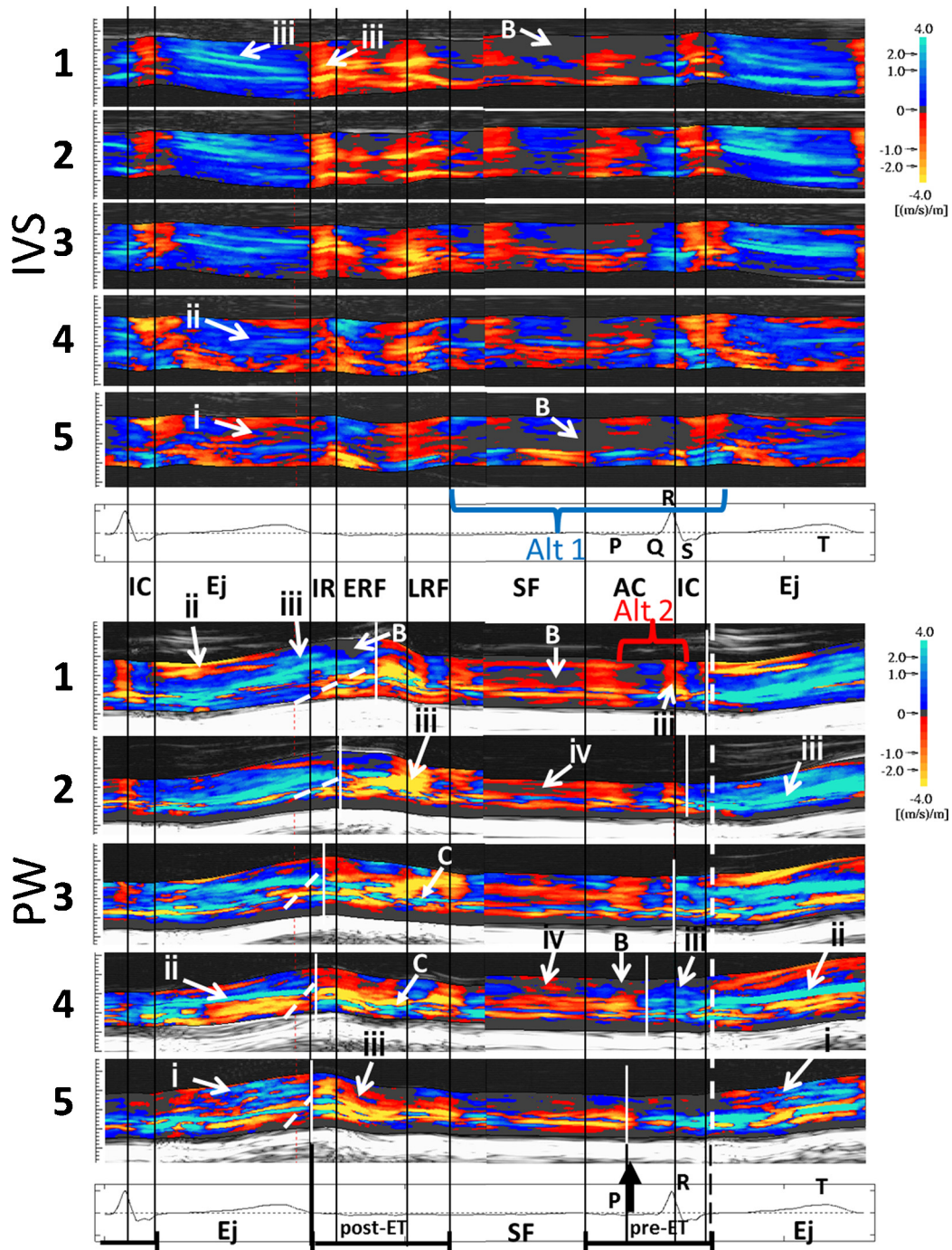


**Fig. 2.** M-mode images of the strain rate (SR) distribution in the interventricular septum (IVS) and posterior wall (PW) during one cardiac cycle. Nos. 1–5 were obtained with the beam direction 1–5 in the upper graphic in Fig. 1. The cold color area shows an increment of the SR (contracting) and the warm color area decrement (extending). The color bar demonstrates the grade of the SR. Large black arrow, beginning of the PW contraction; white narrow broken oblique lines, beginning of the PW extension; c, contracting muscle component; white narrow vertical lines, beginning and ending of the PW contraction; i, spotted distribution; ii, multi-layered distribution; iii, toned distribution (apex (5): cold color, base (1): warm color); iv, stratified distribution; B, black area (relaxation); Alt 1, alternating appearance of the multi-layered distribution; Alt 2, alternating appearance of the toned distribution; IC, isovolumetric contraction; Ej, ejection; IR, isovolumetric relaxation; ERF, early stage rapid filling; LRF, late stage rapid filling; SF, slow filling; AC, atrial contraction; pre-ET, pre ejection transitional phase; post-ET, post ejection transitional phase.

contraction propagated toward the base until the anterior half of the early rapid filling phase (ERF).

During the contraction, 3 distribution patterns were demonstrated (Fig. 2, bottom), that is, the spotted distribution (i) at the apical part, the multi-layered distribution (ii) at the central and basal parts, and the toned distribution (iii) at the basal part.

The extension began at the apical epicardial side, coinciding in time with the T wave of ECG (dashed white lines), and propagated

toward the endocardial side, and finally reaching the ERF. Thereafter, the process continued to the phase of end of pre-ET through the phase of slow filling (SF). Thus, the contraction was present even in the timing of classic “diastole”.

During the extending period, 2 patterns were also observed from the apical part to the basal part, *i.e.*, the toned distribution (iii) in the phase of post-ET, and the stratified distribution (iv) in the phase of SF.

**Table 1**  
Summary of the SR distribution patterns demonstrated in various cardiac phases (pre-ET, Ej, post-ET, SF) observed at the apical (Ap), central (Cent) and basal (Bas) parts of the IVS and PW.

	Pre-ET	Ej	Post-ET	SF
<i>IVS</i>				
(1) Bas.	iii: Toned (Alt 2)	iii: Toned	iii: Toned	iv: Stratified
(3) Cent.	iii: Toned (Alt 2)	ii: Multi-layered	iii: Toned	iv: Stratified
(5) Ap.	ii: Multi-layered (Alt 1)	i: Spotted	ii: Multi-layered (Alt 1)	ii: Multi-layered (Alt 1)
<i>PW</i>				
(1) Bas.	iii: Toned (Alt 2)	ii: Multi-layered	ii: Multi-layered	iv: Stratified
(3) Cent.	iii: Toned (Alt 2)	iii: Toned		
(5) Ap.	iii: Toned	ii: Multi-layered	i: Spotted	iv: Stratified
		i: Spotted	iii: Toned	iv: Stratified

Alt 1: alternating appearance of the multi-layered distribution; Alt 2: alternating appearance of the toned distribution.

In the pre-ET, the toned distribution was alternatively observed during either contraction or extension (Alt 2).

Furthermore, the string-shaped contracting pattern (C of 3 and 4 in Fig. 2) was observed near the epicardium in the mid-PW during the phase of RF through SF, indicating that a superficial contracting muscle group exists at the area near the epicardium from the central to the basal parts, assisting the active dilatation of the LV.

All the while, gentle extension (stratified distribution) of the wall was observed in the phase of SF. At the epicardial side of the apical part, there was relaxation during SF [black area (B): nearly zero SR].

#### Interventricular septum

As shown in Fig. 2, IVS 4 and 5, the apical contraction began at the LV side coincided in time with the end of the P wave of ECG. Following the temporal extension, the contraction propagated toward the right ventricular (RV) side until the ERF. The apical extension coincided with the T wave of ECG and propagated from the LV side to RV side until ERF. Thereafter, the extension continued until the next P wave of ECG and showed the Alt 1 SR distribution at the apical part, and the stratified distribution (iv) at the central part.

During the contracting period, the spotted distribution (i) at the apical part, the multi-layered distribution (ii) at the central part, and the toned distribution (iii) at the basal part were observed.

At the basal part, the contraction began at the P wave of ECG, but in the pre-ET, Alt 2 pattern of the SR distribution was seen. Thereafter, the contraction progressed from the RV side to the LV side during Ej.

The extension began coincidentally with the end of T wave of ECG (Fig. 2, IVS,1) and ca. 35–37 ms prior to the IIa sound.

The extension occurring during the post-ET phase was caused by the expansion of the LV outflow tract in this period, then further progressed with the stratified distribution with B until the AC through SF.

The process of the C–E property within the IVS was not always similar to that of the PW. Especially, the alternating pattern of the (+) and (–) SR (Alt 2) was demonstrated at the central and basal parts as the toned distribution (iii) in the pre-ET phase. At the apical part in IVS, multi-layered distribution (Alt 1) was alternatively seen until the pre-ET phase through the SF.

During the SF, the stratified distribution was observed in the area near the LV side at the basal part. Thus, the characteristics of the C–E property of the IVS were considerably different compared with that in the PW.

#### The myocardial C–E property estimated by the time serial SR distribution

The myocardial C–E property analyzed by the time serial SR distribution showed the following features.

- Both contraction (C) and extension (E) of the wall spread from the epicardial side toward the endocardial side.
- Both C and E began from the apex and spread toward the base.
- The LV contraction began coinciding with the P wave of ECG and continued up to the RF phase in the PW. The extension began at the T wave of ECG and continued to the IC.
- The length of the contracting process and that of the extending process had nearly equal duration.
- In every 5 parts of the IVS, the beginnings of the (+)SR or (–)SR were nearly the same during one cardiac cycle. On the contrary, the beginning and ending of the (+)SR or (–)SR of the PW were quite different through 5 parts as shown by the narrow white vertical lines in Fig. 2. The time delay of the apical part became bigger toward the base.
- During one cardiac cycle, cardiac phases composed of the isolated contraction, isolated extension, and another 2 transitional phases were observed. During the transitional phases, both the contracting state and extending state were observed simultaneously in the different parts of the ventricular wall (Figs. 2 and 4).
- One cardiac cycle was then logically divided into 4 phases: pre-ejection transitional phase (pre-ET), ejection phase (Ej), post-ejection transitional phase (post-ET), and slow-filling phase including the atrial contraction (SF).

#### Discussion

First of all, it should be kept in mind that the usual physiologic terms are not valid in the present article. The former cardiac physiology defined the contraction as mainly the systolic event and the relaxation as solely the diastolic event except atrial systole.

In our study, the term of “contraction” means the positive strain rate of muscle fiber, irrespective of the timing throughout the cardiac cycle, and does not necessarily mean the previously defined systole. This contraction does exist during conventional diastole. The counterpart is “extension” which has a negative SR, in which the muscle fiber is not in the static state, but in active extension. Conventionally, the extension may be called diastole, but the extension does occur even during classic systole.

In between, there is the time when the muscle fiber is in neither contraction nor extension, *i.e.* the SR is near zero, and the hue in Fig. 2 is black. This is defined as “relaxation” in this paper, and is seen during diastole, but may be observed in several timings during the cardiac cycle.

As far as we are aware, there are no published articles similar to the present study that deal with the microscopic observation of the physiological aspects of cardiac muscle fiber. This is due to the lack of adequate *in situ* methodology to monitor cardiac muscle

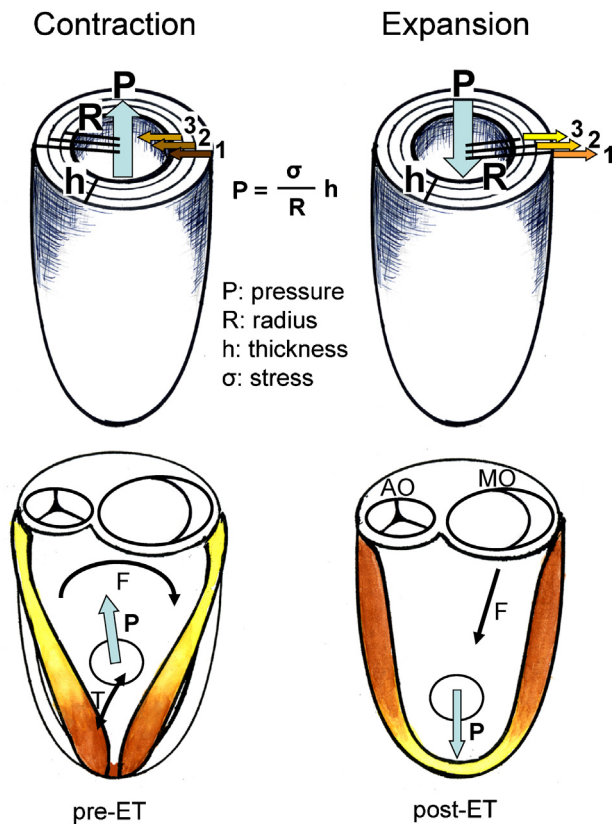


**Fig. 3.** Schematic representation of the propagation of C–E in the left ventricular (LV) wall. Top: in the contracting process, the “*h*” (wall thickness) gradually increases, then the front of contraction progress from 1 to 3, and the *R* (radius) will decrease from 1 to 3. Accordingly, the power produced is easily centralized to the central area of the LV and the positive pressure increases (left figure: contraction). In the extending process, both the “*h*” and the “*R*” are reversed and negative pressure increases (right figure: relaxation, expansion). Bottom: schematic representation of the distribution of contraction and extension in the myocardium at the pre-ET and post-ET phases of the LV wall. Yellow area is in the extending state and brown area in the contracting state. Blue arrow (*P*), pressure; black arrow (*F*), expected blood flow direction; pre-ET, pre-ejection transitional phase; post-ET, post-ejection transitional phase; MO, mitral orifice; AO, aortic orifice; T, tension appeared in the endocardial area in the posterior wall.

contraction and extension. In this regard, the methodology in the present study, *i.e.* the phase difference tracking method for measuring the high resolution SR appears to be extremely valuable. It is because the accurate measurement of SR distribution is considered to reflect the performance at the sarcomere level and to indicate the contractility or extensibility in the muscle fiber level.

The microscopic study disclosed that the myocardial contraction or extension does occur asynchronously, leading to the uniformity in all muscle fibers of the wall. Their timing and also magnitude were different in the parts of the ventricular wall. For example, during the apical contraction, the base was in the state of extension, and the events in the epicardial side differed from that of the endocardial side. Therefore, generally speaking, the contracting process and the extension process coexist independently during the same cardiac phase. Despite this complexity, the SR distribution showed some regularities in the onset and magnitude of the SR at the basal parts of the PW and the IVS during Ej.

The beneficial effects on the cardiac muscle function evidenced by the C–E property studied by the SR distribution were as follows:

1) Propagation and integration of the C–E from the epicardial side to the endocardial side

This propagation behavior [16] is important in that the force of contraction becomes stronger as the propagation progresses

toward the endocardium by the integration of the contraction. In addition, the concave shape of the LV internal surface acts as a centralizer of the power produced by the contraction or the extension (Fig. 3, top). When the radius (*R*) changes from 1 to 3, the thickness (*h*) will increase proportionally, giving greater power of contraction.

Assuming that the contractility or extensibility per unit volume of the muscle tissue is constant, the simple Laplace equation ( $P = \sigma \cdot h / R$ , where *P* is intraventricular pressure,  $\sigma$  is stress of the wall, *h* is wall thickness, and *R* is internal radius) [1,19] indicates the pressure (*P*) either rapidly increases in the contracting process or rapidly decreases in the expanding process.

2) Propagation of the C–E from the apex to the base

During isovolumetric contraction (IC) and isovolumetric relaxation (IR), it has been supposed that the ventricular muscles are in the static state. However, there was definite contraction or extension as evidenced by the SR distribution, *i.e.* blood flow develops even during these phases.

As demonstrated in the bottom diagram of Fig. 3, during pre-ET, the SR distribution clarified that the contraction at the apical part accompanied with the simultaneous basal extension. This indicates that the pressure change (*P*) primarily occurs at the apex, and immediately transmits toward the outflow or inflow tract, and thus the basal blood flow is obliged to change. The basal part expanded and the rotating flow is produced during IC [17]. While in post-ET, the apical part relaxed while the basal part contracted, giving downward flow in the ventricle during IR [20].

3) Energy consumption of the ventricular muscle

Although the contracting part (*e.g.* apex) and the extending part (*e.g.* base) are observed simultaneously, the time delay of both parts is clear in the PW, but not so in the IVS. This implies that the contracting energy positively extends the relaxing part to save energy consumption due to the muscle contraction.

4) Peristalsis and bellows action of the LV

The propagation sequence of contraction or extension from the apical to basal part inevitably produces the peristalsis of the PW, whereas the difference of the C–E between PW and IVS produces the bellows action of the LV.

The peristalsis and the bellows action of the PW seem to cause the squeezing effect [17] to the intraventricular blood during Ej (aortic ejection [21]) and the suction effect [20] to the inflow blood during RF (mitral inflow). In this sequence, the importance is that the PW and the IVS have different but interacting contributions to the LV pump function.

5) A new division of the cardiac phase

The overwhelming importance of the present study is the confirmation of 4 newly identified cardiac phases, which have never been proposed by any previous cardiac physiologists [1–3,8]. The contraction and the extension of the LV wall are not independent events, but interact dependently upon each other. This conclusion is based on the definite observation of the SR distribution during the transitional phases, in which both contraction and extension are observed at the same time. In this respect, we finally categorized the 4 cardiac phases including the pre-ET and post-ET transitional phases as shown in Fig. 4.

Surprisingly enough, the sum of the duration of total contraction and that of total extension are nearly equal at least in normal subjects. This may indicate that the LV is able to have smooth movement like a rotary pump without giving a specific load in any areas of the LV muscle. This assumption is particularly important to conditions such as the crisis of the sudden change in the pressure, volume, or an accelerated heart rate by keeping smooth muscular action and thus adequate pump function continuously.

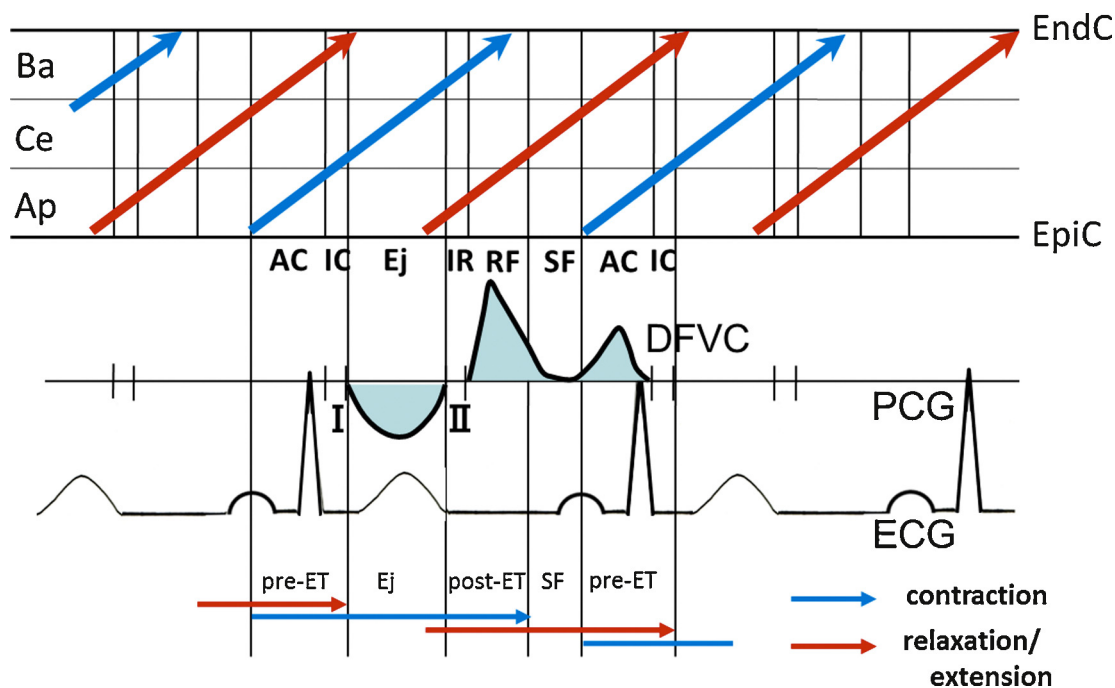


**Fig. 4.** Schematic representation of the contraction–extension (C–E) property of the left ventricular wall (upper graph), and schematic display of the correlation among C–E property, electrocardiogram (ECG), Phonocardiogram (PCG), Doppler flow velocity curve (DFVC, blue colored curve) and the timing of the contraction and extension (lower graph). Upper graph: red thick arrows, extending process; blue thick arrows, contracting process; Ba, basal part; Ce, central part; Ap, apical part; EndC, endocardial part; EpiC, epicardial part; AC, atrial contraction; IC, isovolumetric contraction; IR, isovolumetric relaxation; RF, rapid filling; SF, slow filling. Lower graph: pre-ET, pre-ejection transitional phase; Ej, ejection; post-ET, post-ejection transitional phase; I, 1st heart sound; II, 2nd heart sound.

## Limitations

Although the results were similar in all cases, the sampling was small, so that further accumulation of normal as well as pathological data may be needed to reach the final conclusions. At present, the examination was off-line which required a long time for the analysis. In future, this should be replaced by on-line to alleviate the time loss of examination.

The technology of “phase difference tracking method in ultrasonics” is not widely recognized because it was developed in our laboratory; therefore, the understanding of our results might be difficult. We welcome candid criticism and will accept any questions.

## Conclusions

The new method for measuring the SR distribution in the LV myocardium was introduced to analyze the C–E property of the cardiac muscle noninvasively with high spatial resolution.

There was no synchronous contraction or extension of the LV muscles, and the time serial SR distribution during cardiac cycle disclosed the C–E property of the myocardium *in situ*, where independent contraction or extension was evident through the cardiac cycle. The PW and the IVS had a different C–E property and gave the peristalsis and bellows action.

The harmonious succession of the 4 newly identified cardiac phases seemed to be of help to understand the mechanism of keeping long-lasting pump function of the LV.

## References

[1] Ishida N, Takishima T. Dynamics of the myocardium. *Cardiodynamics and its clinical application*. 2nd ed. Tokyo: Bunkodo Co.; 1992. p. 1–63.

- [2] Braunwald E, Sonnenblick EH, Ross Jr J. Contraction of the normal heart. In: Braunwald E, editor. *Heart disease*, vol. I, 2nd ed. Philadelphia: WB Saunders & Co.; 1984. p. 409–46.
- [3] Matsuda K, editor. *Japanese handbook of physiology*, vol. III. Physiology of circulation. Tokyo: Igakushoin Ltd.; 1969. p. 70–147.
- [4] Barnett VA. Cardiac myocytes. In: Iuzzo PA, editor. *Handbook of cardiac anatomy, physiology and devices*, Part III. Totowa, NJ: Humana Press Inc.; 2005. p. 113–21.
- [5] Sonnenblick EH, Ross Jr J, Covell JW, Spotnitz HM, Spiro D. The ultrastructure of the heart in systole and diastole: changes in sarcomere length. *Circ Res* 1967;21:423–31.
- [6] Brutsaert DL, Sys SU. Relaxation and diastole of the heart. *Physiol Rev* 1989;69:1228–315.
- [7] Brutsaert DL, DeClerk NM, Goethals MA, Housmans PR. Relaxation of ventricular cardiac muscle. *J Physiol* 1978;283:469–80.
- [8] Rushmer RF. Functional anatomy and control of the heart. In: *Cardiovascular dynamics*. 4th ed. Philadelphia: WB Saunders & Co.; 1970. p. 76–131.
- [9] Sato Y, Maruyama A, Ichihashi K. Myocardial strain of the left ventricle in normal children. *J Cardiol* 2012;60:145–9.
- [10] Nishimura K, Okayama H, Inoue K, Saito M, Yoshii T, Hiasa G, Sumimoto T, Inaba S, Ogimoto A, Funada J, Higaki J. Direct measurement of the radial strain in the inner-half layer of the left ventricular wall in hypertensive patients. *J Cardiol* 2012;59:64–71.
- [11] Suzuki K, Akshi Y, Mizukoshi K, Kou S, Takai M, Izumo M, Hayashi A, Ohtani E, Nobuoka S, Miyake F. Relationship between left ventricular ejection fraction and mitral annular displacement derived by speckle tracking echocardiography in patients with different heart diseases. *J Cardiol* 2012;60:55–60.
- [12] Tanaka M, Kanai H, Sato M, Chubachi N. Moving velocity measurement in the local myocardial tissue by the phase difference tracking method. *J Cardiol* 1996;28(Suppl. I):163.
- [13] Kanai H, Hasegawa H, Chubachi N, Koiwa Y, Tanaka M. Noninvasive evaluation of local myocardial thickening and its color-coded imaging. *IEEE Trans Ultrason Ferroelect Freq Contr* 1997;44:752–68.
- [14] Kanai H, Hasegawa H, Chubachi N, Koiwa Y, Tanaka M. Non-invasive evaluation of spatial distribution of local instantaneous strain energy in heart wall. In: Lees S, Ferrari LA, editors. *Acoustic imaging*. New York: Plenum Press; 1997. p. 187–92.
- [15] Yoshiara H, Hasegawa H, Kanai H, Tanaka M. Ultrasonic imaging of propagation of contraction and relaxation in heart walls at high temporal resolution. *Jpn J Appl Phys* 2007;46:4889–96.
- [16] Kanai H, Tanaka M. Minute mechanical-excitation wave-front propagation in human myocardial tissue. *Jpn J Appl Phys* 2011;50, 07HA01-7.

- [17] Tanaka M, Sakamoto T, Sugawara S, Nakajima H, Katahira Y, Ohtsuki S, Kanai H. Blood flow structure and dynamics, and ejection mechanism in the left ventricle: analysis using echo-dynamography. *J Cardiol* 2008;52: 86–101.
- [18] Tanaka M, Dunn F. Acoustic properties of the fibrous tissue in myocardium and detectability of the fibrous tissue by echo method. In: Dunn F, Tanaka M, Ohtsuki S, Saijo Y, editors. *Ultrasonic tissue characterization*. Tokyo: Springer-Verlag; 1996. p. 231–43.
- [19] Yin FCP. Ventricular wall stress. *Circ Res* 1981;49:829–42.
- [20] Tanaka M, Sakamoto T, Sugawara S, Nakajima H, Katahira Y, Kameyama T, Kanai H, Ohtsuki S. Physiological basis and clinical significances of left ventricular suction studied using echo-dynamography. *J Cardiol* 2011;58: 232–44.
- [21] Tanaka M, Sakamoto T, Sugawara S, Nakajima H, Kameyama T, Katahira Y, Ohtsuki S, Kanai H. Spiral systolic blood flow in the ascending aorta and aortic arch analyzed by echo-dynamography. *J Cardiol* 2010;56:97–110.